

Dynamics and energy spectra of aperiodic discrete-time quantum walks

C. V. Ambarish,¹ N. Lo Gullo,² Th. Busch,³ L. Dell'Anna,⁴ and C.M. Chandrashekar^{1,5}

¹*The Institute of Mathematical Sciences, C. I. T. Campus, Taramani, Chennai 600113, India*

²*Department of Physics, University of Milan, Italy*

³*Okinawa Institute of Science and Technology Graduate University, 904-0495 Okinawa, Japan*

⁴*Department of Physics and Astronomy, University of Padua, Italy*

⁵*Homi Bhabha National Institute, Training School Complex, Anushakti Nagar, Mumbai 400094, India*

Deterministically aperiodic sequences are an intermediary between periodic sequences and completely random sequences. Materials which are translationally periodic have Bloch-like extended states, while random media exhibit Anderson localisation. Materials constructed on the basis of deterministic aperiodic sequences such as Fibonacci, Thue-Morse, and Rudin-Shapiro exhibit different properties, which can be related to their spectrum. Here, by investigating the dynamics of discrete-time quantum walks using different aperiodic sequences of coin operations in position space and time we establish the role of the diffraction spectra in characterizing the spreading of the wavepacket.

I. INTRODUCTION

Quantum walks are the quantum-mechanical analogue of classical random walks and just like their classical counterparts, the two variants exist: discrete-time quantum walks (DTQWs) [1] and continuous-time quantum walks (CTQWs) [2]. They have played an important role in the field of quantum information processing as powerful parts of quantum algorithms [3, 4] and have been shown to be a universal quantum computation primitive; in that any quantum computation can be realized efficiently [5, 6]. Furthermore, with the ability to engineer quantum walks by controlling the parameters of the evolution operators, quantum effects such as localization [7, 8] and topological bound states [9] have been simulated. Controlled dynamics of quantum walks have also allowed to simulate relativistic quantum dynamics where the speed of light is mimicked by the parameter in the evolution operator [10–14]. Their versatility and ease of implementation in physical systems such as, NMR [15, 16], trapped ions [17, 18], atoms [19, 20] and photonic systems [21, 22] makes them promising candidates to explore and engineer quantum dynamics beyond the Schrödinger equation.

Among the two variants of quantum walks, DTQWs are defined for a particle with an internal degree of freedom, to which the quantum coin operations are applied. These quantum coin operations can be position and time-dependent, which can lead to deviations from quadratic spreading of the wavepacket [23], including the emergence of Anderson localisation [24] for a completely disordered arrangement of coin operations in position space and/or time [7, 25]. It is therefore natural to wonder about the behavior of DTQWs when the coin operation is aperiodic in nature [26]. Studies of the behavior of DTQWs for coin operations that are arranged in the aperiodic Fibonacci sequence [26] have already found a diffusive behavior without any signature of localization [27, 28]. However if this behavior is limited to just this sequence or extends to other aperiodic sequences as well is not yet

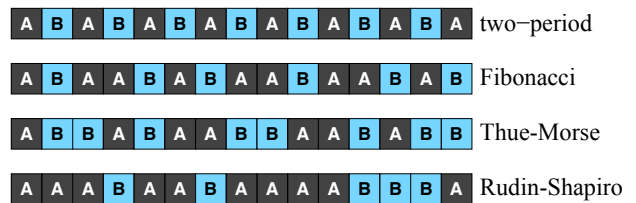


FIG. 1: (Color online). Schematic of the arrangement of the two values for the two-periodic and the deterministic aperiodic sequences.

clear.

Below we will first briefly introduce the deterministic aperiodic sequences that we will study and that have previously been of great interest in condensed matter physics, photonics and material sciences [29, 30].

Materials with deterministic aperiodic sequences can be thought of as *in between* materials with long-range translational symmetry (crystals) and amorphous materials with no long range order. Quasicrystals are one example [31] and searching for other non-periodic materials that have a crystal-like spectrum is an active research area. Of particular interest in this field have been structures based on the Fibonacci sequence [32, 33], the Thue-Morse sequence [34] and the Rudin-Shapiro sequence [35]. The Fibonacci quasicrystal [32, 33], a 1-D version of the celebrated Penrose tiles, has been studied in great detail because it has a pure-point spectrum. Thue-Morse crystals were shown to have a singular continuous spectrum [34] and the Rudin-Shapiro crystals have a fully continuous spectrum [35]. Several measures have been proposed to quantify the amount of order in aperiodic sequences, for instance based on entropy [36, 37], log-entropy [38] and the structure of the energy-spectrum [39]. In Fig. 1 we show a schematic of the different aperiodic sequences.

Here we study the dynamics of the DTQW with spatial and temporal dislocations in the coin operator based on the three deterministically aperiodic sequences men-

tioned above: the quasiperiodic Fibonacci sequence, critical Thue-Morse sequence and the Rudin-Shapiro sequence. We compare our results with the ones for a standard two-periodic sequence of the form ABAB... and show that the support of the diffraction pattern plays a crucial role in determining the spreading properties of the quantum walker. By studying their energy spectra and their asymptotic behavior we show that the DTQW using the Fibonacci sequence, which has pure point spectrum, shows diffusive spreading behavior similar to the periodic walks. The Rudin-Shapiro sequence, which has a continuous spectrum, shows prominent localization behavior which is closer to a walk with a random coin sequence. Quantum walks using the Thue-Morse sequence with a singular-continuous spectrum comprise of both, diffusing and localized component in the dynamics.

The manuscript is organized as follows. In Section II we briefly review the DTQW and in Section III we introduce the different sequences of aperiodic walks with position and time dependent coin operations. In Section IV and Section V we present the study of energy spectra and the spreading of the walk for all configurations. In Section VI we present the asymptotic behaviour and conclude in Section VII.

II. DISCRETE-TIME QUANTUM WALK

The one-dimensional DTQW is defined on a position space and an internal (coin) space. The position space is spanned by the basis vectors $|x\rangle$, with $x \in \mathbb{Z}$, and the internal space of the particle is a two dimensional space spanned by $|\uparrow\rangle = \begin{pmatrix} 1 \\ 0 \end{pmatrix}$ and $|\downarrow\rangle = \begin{pmatrix} 0 \\ 1 \end{pmatrix}$. Each step of the walk consists of the application of one coin and one shift operator. The coin operator is unitary and can be written as

$$\hat{C}(\theta) = \begin{pmatrix} \cos(\theta) & -\sin(\theta) \\ \sin(\theta) & \cos(\theta) \end{pmatrix}. \quad (1)$$

The shift operator performs the translation in the position space conditioned on the internal degree of freedom of the walker and can be written as

$$\hat{S} = \sum_{x=-N}^N |\uparrow\rangle \langle \uparrow| \otimes |x-1\rangle \langle x| + |\downarrow\rangle \langle \downarrow| \otimes |x+1\rangle \langle x|. \quad (2)$$

When the coin operation is homogeneous and time independent, the state of the system after t steps ($t \in \mathbb{N}$) is given by $|\psi_t\rangle = \hat{W}(\theta) |\psi_{t-1}\rangle$ where $\hat{W}(\theta) = \hat{S}(\hat{I} \otimes \hat{C}(\theta))$. In the following we will consider the situation where the coin operator can have two values, θ_1 and θ_2 , and is either time dependent but homogeneous in space or inhomogeneous in space and constant in time.

III. APERIODIC QUANTUM WALKS WITH POSITION AND TIME DEPENDENT COIN OPERATIONS

In this section we will first introduce the sequences of the coin operations for the aperiodic settings we are going to study and then calculate the spread in the probability distribution after a certain time t . As a reference, we will also consider a DTQW with a regular distribution of two coins, which we will call a two-period sequence. For all walks we will fix $\theta_1 = \pi/4$ and study the dynamics for different values of θ_2 .

The support of the diffraction pattern plays a crucial role in determining the spreading properties of the walker. According to the Lebesgue theory of measure the support can be decomposed into a pure-point, singular continuous and absolutely continuous components. The Fibonacci, Thue-Morse and Rudin-Shapiro quasicrystals are particularly well suited to study the role of each of these components, since their diffraction measures have pure-point, singular continuous and absolutely continuous support, respectively. On the other hand it has also been shown that their energy spectra are all singular continuous [39, 40].

A. Periodic and aperiodic sequences

Two-periodic sequence: The two-period sequence is of the form ABABAB.....AB and it is the base sequence we will use to compare the deterministic aperiodic sequences to.

Fibonacci sequence: The Fibonacci sequence of two elements is defined by the substitution rule $A \rightarrow AB$ and $B \rightarrow A$, which can recursively be written as $S_{N+1} = S_N S_{N-1}$ ($S_1 = B, S_2 = A$).

Thue-Morse: The Thue-Morse sequence of two elements is defined by the substitution rule $A \rightarrow AB$ and $B \rightarrow BA$ or recursively as $S_{N+1} = S_N \overline{S_N}$ ($S_1 = A$), where $\overline{S_N}$ is the string S_N in which the two letters A and B have been exchanged.

Rudin-Shapiro: The Rudin-Shapiro sequence is defined by a four-element substitution sequence with the rules given by $P \rightarrow PQ, Q \rightarrow PR, R \rightarrow SQ$ and $S \rightarrow SR$. To obtain a sequence composed of only two elements, A and B , we perform the mapping $(P, Q) \rightarrow A, (R, S) \rightarrow B$.

B. Position dependent coin operations

By defining the states $|\nearrow_x\rangle = \hat{C}(\theta(x)) |\uparrow\rangle$ and $|\searrow_x\rangle = \hat{C}(\theta(x)) |\downarrow\rangle$, we can rewrite the single step evolution operator $\hat{W} = \hat{S}\hat{C}'$ as

$$\hat{W} = \sum_{x=-N}^N |\uparrow\rangle \langle \nearrow_x| \otimes |x-1\rangle \langle x| + |\downarrow\rangle \langle \searrow_x| \otimes |x+1\rangle \langle x|. \quad (3)$$

This allows us to interpret the evolution of the system as an itinerant spin in an inhomogeneous magnetic field and we expect the mobility of the spin to be related to the spatial structure of the chosen sequence. To see this let us consider the single step evolution operator $U = S \otimes C'$ where

$$\hat{S} = \sum_{x=-N}^N |\uparrow\rangle \langle \uparrow| \otimes |x-1\rangle \langle x| + |\downarrow\rangle \langle \downarrow| \otimes |x+1\rangle \langle x|$$

$$\hat{C}' = \sum_{x=-N}^N |x\rangle \langle x| \otimes \hat{C}(\theta(x)).$$

Because $\theta(x)$ can only have two values, θ_1 or θ_2 , we can partition the whole lattice \mathcal{L} into two sublattices \mathcal{L}_1 and \mathcal{L}_2 such that $\mathcal{L} = \mathcal{L}_1 \cup \mathcal{L}_2$ where $\mathcal{L}_i = \{x : \theta(x) = \theta_i\}$.

Using this observation we can rewrite

$$\hat{C}' = \sum_{x=-N}^N |x\rangle \langle x| \otimes \left(\hat{C} + w(x)\Delta\hat{C} \right), \quad (4)$$

where $\hat{C} = (C(\theta_1) + \hat{C}(\theta_2))/2$, $\Delta\hat{C} = (\hat{C}(\theta_1) - \hat{C}(\theta_2))/2$ and $w(x) = 1 \quad \forall x \in \mathcal{L}_1$ and $w(x) = -1 \quad \forall x \in \mathcal{L}_2$. The function $w(x)$ encodes the information on the geometry of the original spatial distribution of the two coins regardless of the actual form of the coin operators.

Specifically, in this form it is clear that the dynamics of the walker is linked to the underlying geometric distribution of the letters A and B of the sequence used. To see this let us introduce the states $|k\rangle$ such that $\langle x|k\rangle = e^{-ixk}/\sqrt{L}$ with $L = 2N + 1$ and the identity (for the spatial part) in this basis being $\hat{\mathbf{1}} = \int dk |k\rangle \langle k|$. This allows us to write

$$\hat{C}' = \int dk |k\rangle \langle k| \otimes \hat{C} + \int dk dq \tilde{f}(k-q) |k\rangle \langle q| \otimes \Delta C \quad (5)$$

where

$$\tilde{f}(q) = \frac{1}{L} \sum_{x=-N}^N e^{iqx} w(x). \quad (6)$$

The Fourier amplitudes $\tilde{f}(q)$ are nothing but the amplitudes of the diffraction spectrum of the weighted Dirac comb $\omega = \sum_x w(x)\delta_x$.

C. Time dependent coin operations

To study the effect of temporally dependent coin operation we consider the application of $\hat{W}(\theta(t))$ at the t^{th} time step where $\theta(t)$ is chosen according to the distribution of $A \rightarrow \theta_1$ and $B \rightarrow \theta_2$ in the chosen sequence. For instance, if the chosen string is $ABABBBAAABB$,

then after $t = 6$ time steps the evolution operator will be $\hat{U} = \hat{W}(\theta_2)\hat{W}(\theta_2)\hat{W}(\theta_2)\hat{W}(\theta_1)\hat{W}(\theta_2)\hat{W}(\theta_1)$.

Similar to the case of the position dependent coin we can define states $|\nearrow_t\rangle = \hat{C}(\theta(t))|\uparrow\rangle$ and $|\swarrow_t\rangle = \hat{C}(\theta(t))|\downarrow\rangle$, which allows us to rewrite the single step evolution operator as

$$\hat{W}(\theta(t)) = \sum_{x=-N}^N |\uparrow\rangle \langle \nearrow_t| \otimes |x-1\rangle \langle x| + |\downarrow\rangle \langle \swarrow_t| \otimes |x+1\rangle \langle x| \quad (7)$$

The total evolution operator connecting the initial state to the state at time step t , namely $\hat{U}(t) = \prod_{s=1}^t \hat{W}(\theta(s))$, can be interpreted as the evolution of a spin in a time dependent magnetic field. In this sense the change in coin operation for each time (change in magnetic field) in the system can be considered as a kicked itinerant spin on a lattice.

IV. ENERGY SPECTRA

In this section we discuss the energy spectra for the DTQWs using the different sequences introduced in preceding section. Here a comment is necessary on what we mean by energy spectrum in this context and how we derive it. In general an operator of the form given in Eq. (3) acting on a finite space is not a unitary operator due to the spatial part. The iterative application of the single step operators therefore results, in general, in a non-probability conserving evolution under a total operator \hat{T} . The latter is such that $\hat{T}\hat{T}^\dagger = \hat{T}^\dagger\hat{T} = \hat{I}$ still acts as a unitary operator in a sub lattice $[-\tilde{N}, \tilde{N}]$ with $\tilde{N} < N$. Therefore, for localized initial states and for a certain t^* such that the probability $p_x = |\langle x, \uparrow | \psi(t^*) \rangle|^2 + |\langle x, \downarrow | \psi(t^*) \rangle|^2$ of finding the walker in at a given position x is $p_x = 0$ if $x \notin [-\tilde{N}, \tilde{N}]$, we can restrict the dynamics of the walker to that interval and consider it as a unitary evolution. The energy spectrum is then the spectrum of the unitary operator \hat{U} which is the restriction of \hat{T} acting onto the above mentioned subspace. It is worth stressing that this is mainly due to the numerical limitations, whereas this problem does not arise in the thermodynamic limit.

The energy spectrum of a homogeneous and time-independent DTQW for the case $\theta = \pi/4$ is shown in Fig. 2. It is given by $\epsilon_n = \imath \log(\lambda_n)$, with the λ_n being the eigenvalues of $\hat{W}(\theta)$, and can be seen to consist of two main bands, each of which is the spectrum of a tight binding Hamiltonian.

The two bands are due to the presence of the internal degree of freedom (coin) and the two extreme cases are (a) $\theta = n\pi$ and (b) $\theta = (2n-1)\pi/2$ which correspond to $C = (-1)^n \hat{I}$ and $C = (-1)^n (|\uparrow\rangle \langle \downarrow| - |\downarrow\rangle \langle \uparrow|)$, respectively. To see this let us consider an infinite lattice ($N \rightarrow \infty$) and introduce the states $|k\rangle$ such that $\langle x|k\rangle = e^{-ixk}/\sqrt{L}$ with $L = 2N + 1$ and the identity

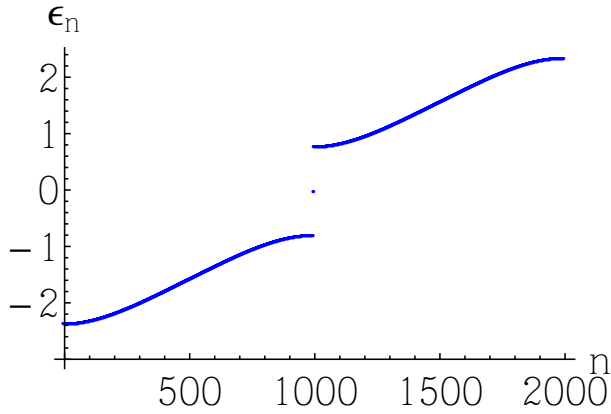


FIG. 2: (Color online). Spectrum $\epsilon_n = \imath \log(\lambda_n)$ where λ_n are the eigenvalues of the operator \hat{W} in Eq. (3) for the case $\theta_1 = \theta_2 = \pi/4$.

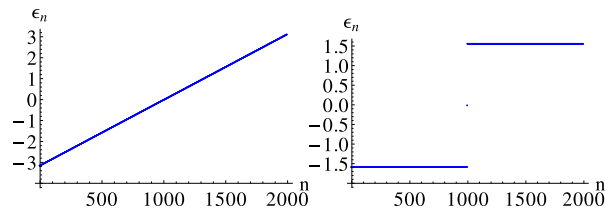


FIG. 3: (Color online). Energy spectra $\epsilon_n = \imath \log(\lambda_n)$ where λ_n are the eigenvalues of the operator $\hat{W}(\theta)$ in Eq. (3), for $\theta = 0$ (left) and $\theta = \pi/2$ (right).

(for the spatial part) in this basis $\hat{\mathbf{1}} = \int dk |k\rangle \langle k|$. This allows us to rewrite the single step evolution operator as

$$\hat{W} = \int dk |k\rangle \langle k| \otimes (e^{-\imath k} |\uparrow\rangle \langle \uparrow| + e^{\imath k} |\downarrow\rangle \langle \downarrow|) \hat{C}(\theta). \quad (8)$$

For the case (a) $C(n\pi) = \pm \hat{I}_C$ the eigenstates of \hat{W} are $|k\rangle |\uparrow\rangle$ and $|k\rangle |\downarrow\rangle$ with eigenvalues $e^{-\imath k}$ and $e^{\imath k}$ respectively. On the other hand in case (b) $\hat{C} = (-1)^n (|\uparrow\rangle \langle \downarrow| - |\downarrow\rangle \langle \uparrow|)$ the eigenstates are given by $e^{\pm \imath \frac{\pi}{2}} \int dk |k\rangle (e^{\imath \frac{k}{2}} |\uparrow\rangle \pm e^{-\imath \frac{k}{2}} |\downarrow\rangle) / \sqrt{2}$ with eigenvalues $\pi/2$ and $-\pi/2$. Therefore the spectrum in case (a) is linear without gap at $\epsilon = 0$ whereas in case (b) it is flat inside the two bands which are separated by a gap $\Delta = \pi$ as shown in Fig. 3.

When it comes to the study of the energy spectra of a DTQWs the distinction between spatial aperiodic sequences and temporal aperiodic ones is important.

A. Position dependent coin operations

In the case of DTQWs with position dependent coin operations ($\theta_2 \neq \theta_1$) distributed according to a given aperiodic sequence the spectrum of the system is the same at all time steps and coincides with that of the single step

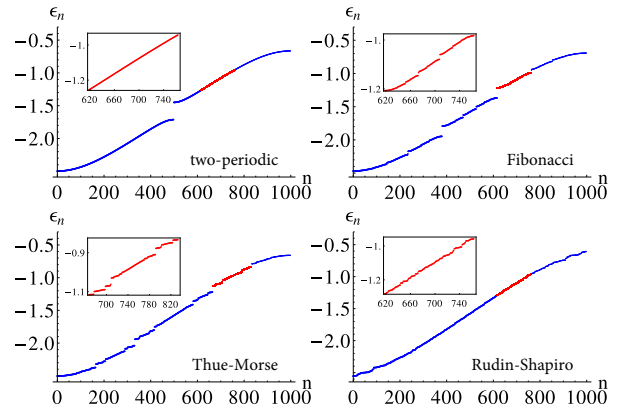


FIG. 4: (Color online). Lowest band of the spectrum $\epsilon_n = \imath \log(\lambda_n)$ where the λ_n are the eigenvalues of the operator $\hat{W}(\theta)$ in Eq. (3). The angles chosen are $\theta_1 = \pi/4$ and $\theta_2 = \pi/6$ and are distributed (from top left to bottom right) according to the two-periodic, the Fibonacci, the Thue-Morse and the Rudin-Shapiro sequence. In the inset of each figure we show a zoomed in part of the spectrum to show the self-similarity of the spectra and the presence of gaps at all energies.

evolution operator $\hat{W}(\theta)$. It can be seen from Fig. 4 that the effect of different coin operations on different sites is to open new gaps inside the two above mentioned main energy bands thus creating sub-bands. The position of these new gaps can be determined in first order perturbation theory (i.e. considering the case $|\theta_2 - \theta_1| \approx 0$) by finding that they open where the intensity of the Fourier transform of $w(x)$ is higher [39–42]. Within the two main bands the structure is therefore determined by the spatial distribution of the two coins and consequently by the geometry of the chosen arrangement.

The above spectra give rise to the densities of states (DOS) shown in Fig. 5, from which key properties of each distribution can be identified. In particular we notice the self-similarity of the energy spectrum of the Fibonacci sequence (top-right) and the broad availability of states for the Rudin-Shapiro sequence throughout the whole sub-band. We also notice that each DOS for all aperiodic arrangements shows singular features (spikes in the DOS), which are a result of the opening of the gaps in the spectrum on a set of zero measure [39, 40]. This translates into plateaus in the integrated DOS.

B. Time dependent coin operations

In the case of DTQW with time dependent coin operations given by aperiodic sequences we deal with a non-autonomous quantum system and therefore we cannot, strictly speaking, define a general energy spectrum. However, we can look at the instantaneous or the asymptotic energy spectrum. Applying different coin operations at different time steps amounts to changing the energy spectrum between two possible spectra in an aperiodic way

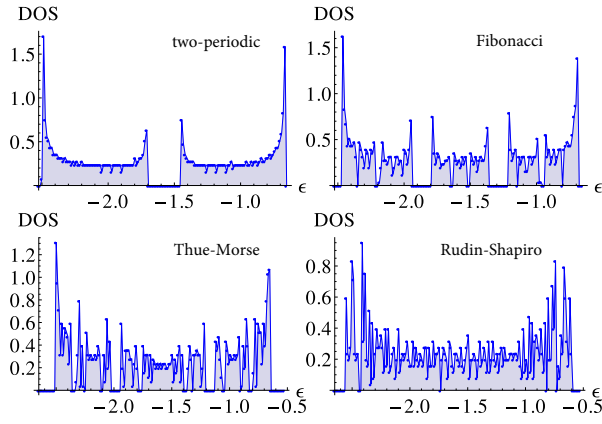


FIG. 5: (Color online). Density of states normalized to the total number of states corresponding to the spectra in Fig. 4. The energy window used to compute these graphs is the same as the one that will be used for the analysis of the asymptotic properties $d\epsilon = 2\pi/t_f$ where $t_f = 500$ is the number of steps.

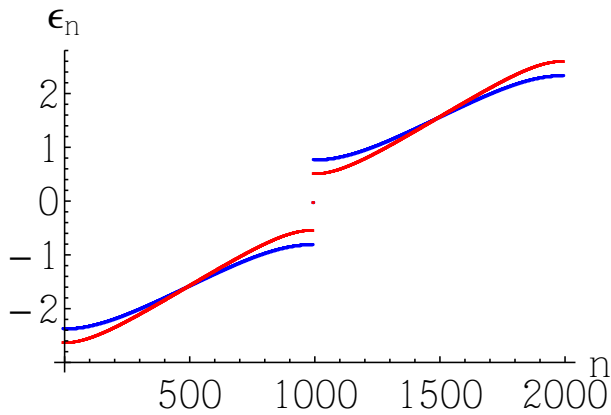


FIG. 6: (Color online). Spectrum $\epsilon_n = i \log(\lambda_n)$ where λ_n are the eigenvalues of the operator $\hat{W}(\theta_1)$ (blue) and $W(\theta_2)$ (red) for the case $\theta_1 = \pi/4$ and $\theta_2 = \pi/6$.

and the two instantaneous energy spectra for the cases $\theta_1 = \pi/2$ and $\theta_2 = \pi/6$ are shown in Fig. 6.

To determine the asymptotic properties of the system it is necessary to look at the spectrum of the total evolution operator $\hat{U}(t)$ for $t \gg 1$. We do this numerically and note that after only a few ($t \approx 30$) steps the spectrum of the total evolution operator does not appreciably change any more. The results for the different sequences are shown in Fig. 7 and one can immediately notice the absence of sub-band gaps, which characterized the spectra in the spatially dependent case. On the other hand, the DOS for the spectrum of the asymptotic evolution operator reveals a much richer structure (see Fig. 8) than what we could have gathered from the spectrum itself. In particular one can note features of the self-similarity for the Fibonacci (top-right) and Thue-Morse (bottom-left) cases. This means that although the single step

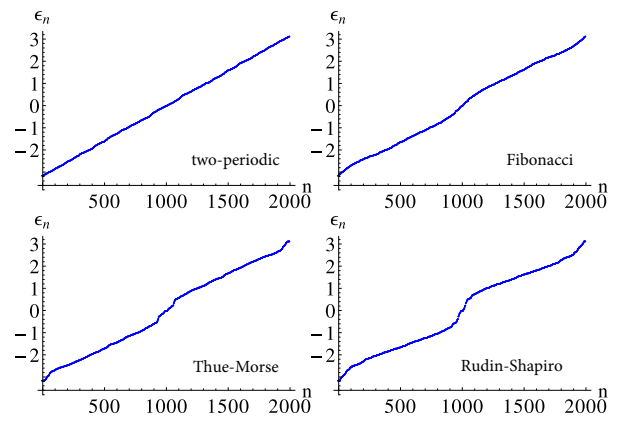


FIG. 7: (Color online). Lowest band of the spectrum $\epsilon_n = i \log(\lambda_n)$ where λ_n are the eigenvalues of the operator $\hat{U}(t)$ with $t = 500$. The angles chosen are $\theta_1 = \pi/4$ and $\theta_2 = \pi/6$.

is completely homogeneous, the aperiodic nature of the temporal distribution arises clearly in the long time limit.

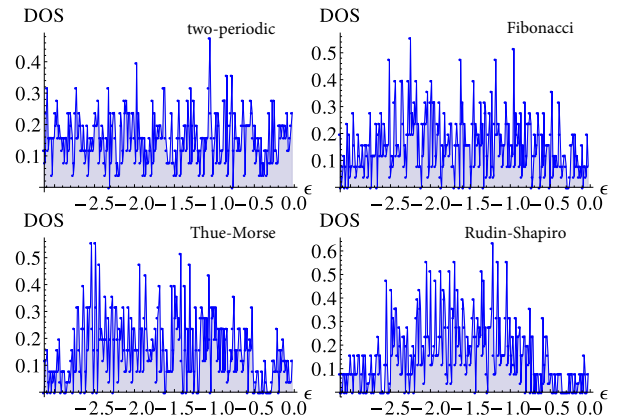


FIG. 8: (Color online). Densities of states normalized to the total number of states and corresponding to the spectra shown in Fig. 7. The energy window used to compute it is the same as the one that will be used for the analysis of the asymptotic properties $d\epsilon = 2\pi/t_f$ where $t_f = 500$ is the number of steps.

V. SPREADING OF THE WALKER

In order to characterize the dynamics of the walker we look at both, the mean displacement $\langle x(t) \rangle$ and its variance given by $\sigma^2(t) = \langle x^2(t) \rangle - \langle x(t) \rangle^2$. We choose the initial state to be $|\psi\rangle = |x=0\rangle \otimes \frac{|\uparrow\rangle + i|\downarrow\rangle}{\sqrt{2}}$, such that the spatial part is localized and the initial coin state as $\theta_1 = \theta_2 = \pi/4$. This leads to a balanced DTQW. In the following we will discuss the different sequences in detail.

Two-periodic: The dynamics of a standard DTQW with a single, fixed coin operator is known to be always

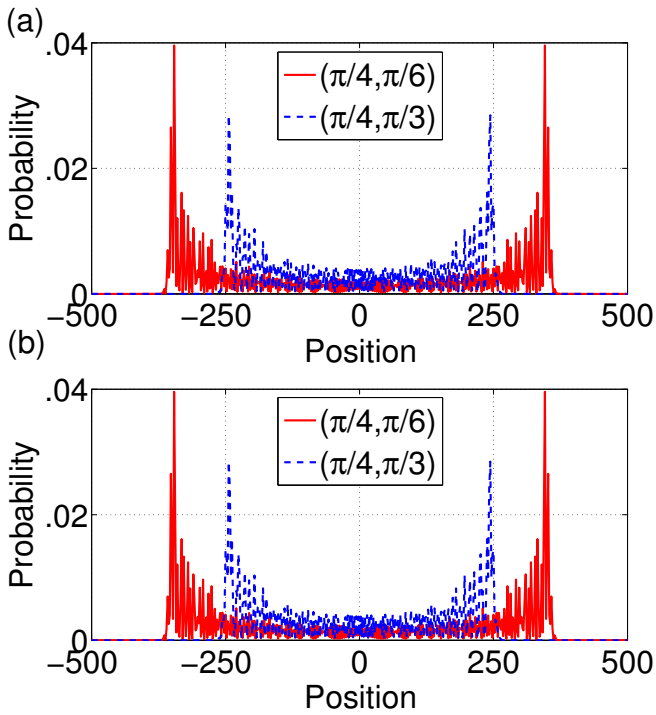


FIG. 9: (Color online). Probability distribution after 500 steps of DTQW using a two-periodic coin for two sets of angles (θ_1, θ_2) . (a) spatial coin dependence (b) temporal coin dependence.

ballistic, with a velocity that depends on θ . From Fig. 9 one can see that this property prevails for the two-period sequence in the temporal as well as in the spatial case, but with the velocity v depending now on θ_1 and θ_2 . This result is not very surprising, since the presence of a periodicity means that localization is absent and therefore the spread in position space has to have the form that has the characteristic peaks in the outer regions.

It is interesting to note that the probability distribution is exactly the same for the spatial and the temporal sequence of the coin operations (compare Figs. 9(a) and (b)). This can be understood by a simple symmetry argument: after t steps the possible positions of the walker range from $-t$ to t , which means that the total number is always odd. Since the sequence is of period two, all even-numbered positions will have one coin and all odd numbered positions have another coin. The structure of the shift operator ensures that at any given time, the amplitude of the walker is either on the odd positions or on the even positions. Therefore only one coin operation is being applied to the walker at any given step, which establishes the equivalence to the temporal two-period walk.

Fibonacci: The probability distributions in position space after 500 steps with the spatial or temporal arrangement of the coin operation given by the Fibonacci sequence are shown in Fig. 10. It is immediately notable that neither walk features the peaks in the outer regions

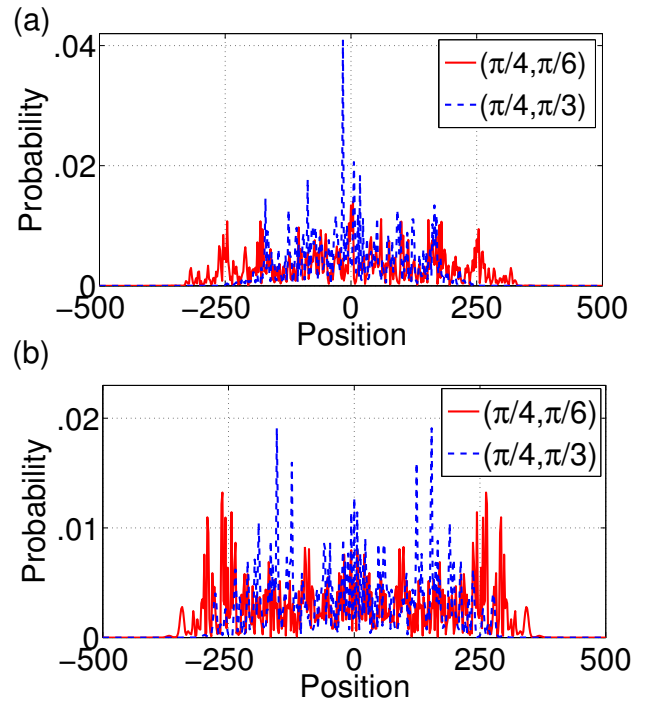


FIG. 10: (Color online). Same as Fig. 9, but using a Fibonacci coin. For both situations the distribution can be seen to be dispersive.

and that no strongly localized peak at origin ($x = 0$) exists. This indicates that the Fibonacci sequence leads to DTQWs with diffusive behaviour.

Thue-Morse: The probability distributions for this sequence are shown in Fig. 11. In the spatial and the temporal case a prominent peak localized at $x = 0$ can be seen, while at the same time a diffusive component is visible as well.

Rudin-Shapiro: The probability distributions for this sequence are shown in Fig. 12. One can see that, compared to the spread for the Fibonacci and the Thue-Morse sequences, the probability distribution for the Rudin-Shapiro sequence is more localized around the origin, $x = 0$. The localization is also stronger for the spatial sequence than for the temporal sequence.

To better understand the different dynamics displayed by the aperiodic walks, we will in the following examine the dynamics as a function of time and the energy spectra of these walks in more detail.

A. Position dependent coin operations

We will first focus on the walks with spatially varying coins and note that while in the standard DTQW evolution the spread of the probability distribution depends on the coin parameter θ [23, 43], its general form is independent of the specific value. We can therefore restrict the parameter space by choosing one of the coins

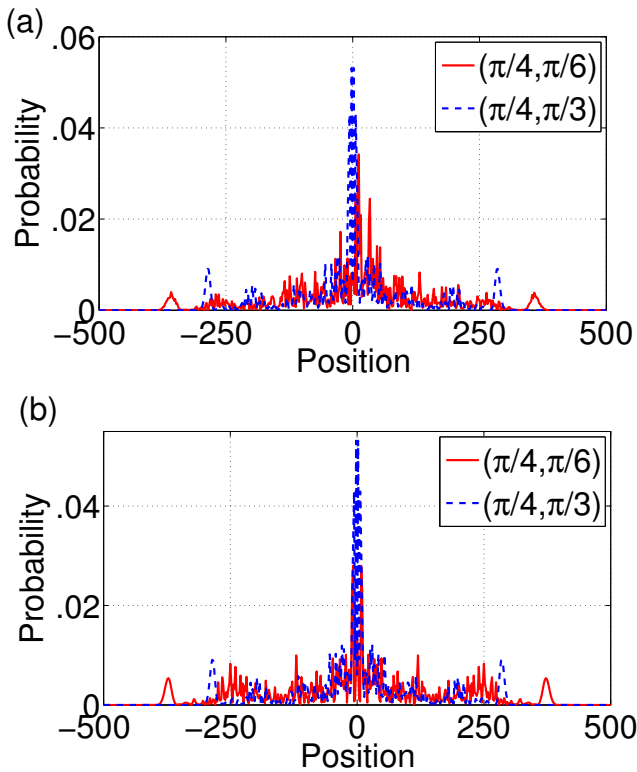


FIG. 11: (Color online). Same as Fig. 9, but using a Thue-Morse coin. For both situations a localized and a diffusing component are visible in the distribution.

to be a Hadamard ($\theta_1 = \pi/4$) and the results we obtain will hold for all values of θ_1 . For all four forms of walks, the standard deviation after 1000 steps and as a function of θ_2 is shown in Fig. 13(a). One can see that the standard deviation for all four sequence is zero when $\theta_2 = \pi/2$ and $3\pi/2$ and maximum and equal when $\theta_2 = \pi/4$ and $3\pi/4$. For all other values, the standard deviation is always highest for two-period walk and lowest for Rudin-Shapiro sequence. For the Fibonacci and the Thue-Morse sequences, the standard deviations are in between these two extremes. For a detailed look into the distributions, we have picked four different values of θ_2 and shown the standard deviation as a function of the number of steps in Figs. 13(b)-(e).

Let us first look at the Fibonacci sequence, which has a pure-point spectrum, and is therefore the closest to a periodic structure. Comparing Figs. 9(a) and 10(a) one can see that the width of the spread in position space is roughly identical for both. However, the standard deviations shown in Figs. 13(b)-(e) show a slower increase for Fibonacci sequence compared to two-periodic sequence. In fact, the difference between them grows with increasing number of steps. Unlike the two-periodic walk, where the peaks in the probability distribution are observed at the outer edges of the distribution, the distribution from the Fibonacci sequence shows larger peaks at multiple

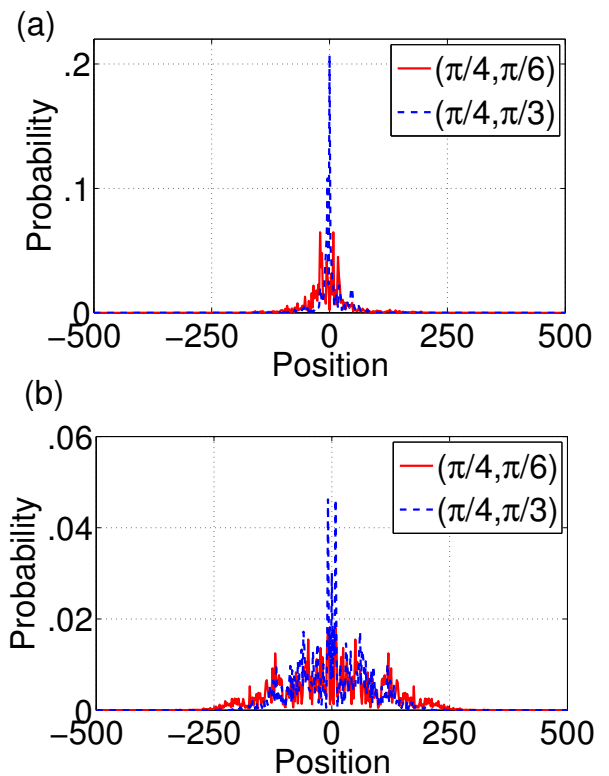


FIG. 12: (Color online). Same as Fig. 9, but using a Rudin-Shapiro coin. The distribution using the spatial sequence is more strongly localized around the origin than the one for the temporal sequence.

spatial positions.

For the walk using the Thue-Morse sequence, which has a singular-continuous spectrum, the probability distribution in Fig. 11 shows that the distribution has both a localized and a diffusing components. The standard deviation as function of number of steps shown in Figs. 13(b)-(e) show that it is smaller than the two-periodic sequence and the Fibonacci sequence.

Finally, the Rudin-Shapiro sequence has an absolutely continuous diffraction spectrum, similar to a completely disordered medium. Here by disorder we mean a random distribution of two values assigned to each point on the lattice. From Figs. 12 and 13(b)-(e) one can see that the distribution localizes around the origin and the value of the standard deviation remains small with increasing number of steps.

B. Time dependent coin operations

The standard deviation of a DTQW with time dependent coin operations after 1000 steps and as a function of θ_2 is shown in Fig. 14(a). One can see that the standard deviation is always lowest for the Rudin-Shapiro sequence, which has the absolutely continuous diffraction

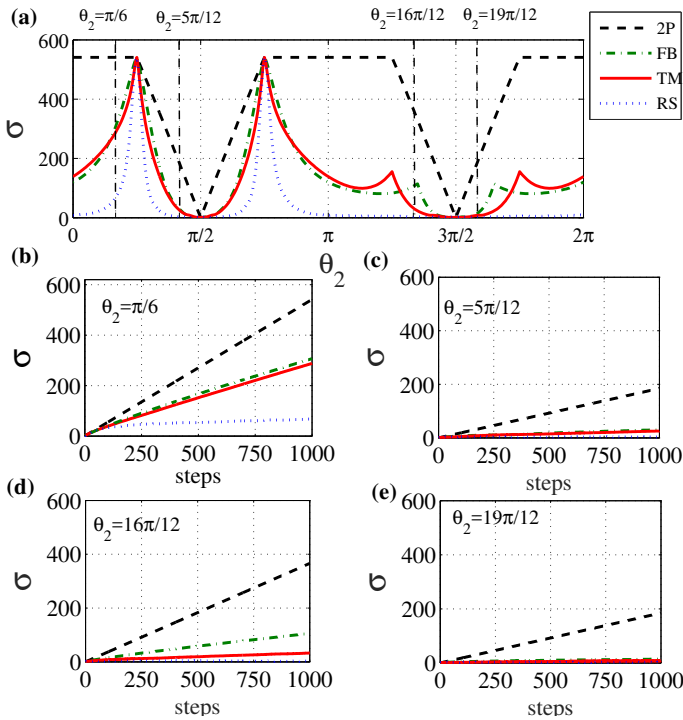


FIG. 13: (Color online). Spatially dependent coin. (a) Standard deviation at the end of a 1000 step walk as a function of θ_2 with $\theta_1 = \frac{\pi}{4}$. (b)-(e) Standard deviation as a function of time for 1000 steps for different values of θ_2 . The notation used for the sequences are 2P \leftrightarrow two-periodic, Fb \leftrightarrow Fibonacci, TM \leftrightarrow Thue Morse, and RS \leftrightarrow Rudin-Shapiro.

spectrum, similar to a completely disordered medium. A detailed look into the development of the deviations is again given for four different values of θ_2 as a function of the number of steps in Figs. 14(b)-(e). One can note that the behaviour is qualitatively similar to the case of the spatially dependent coin, with values for the standard deviation generally higher. This can be understood by noting that it takes a larger number of steps for the system to feel the effects of the aperiodicity.

VI. ASYMPTOTIC BEHAVIOR

We now turn to the characterization of the asymptotic properties of the DTQWs with different coin sequences and will highlight the relation between the asymptotic behavior of the walker distribution and the spectral properties of the chosen aperiodic sequence. In order to make this discussion quantitative we will choose the so-called survival probability or Loschmidt echo $\mathcal{L}(t) = |\nu(t)|^2$ as our figure of merit, which is defined via its amplitude as

$$\nu(t) = \langle \psi(0) | \psi(t) \rangle, \quad (9)$$

where $|\psi(t)\rangle = U(t) |\psi(0)\rangle$.

The reason to consider this quantity is two-fold. On one hand it has a clear physical meaning because it de-

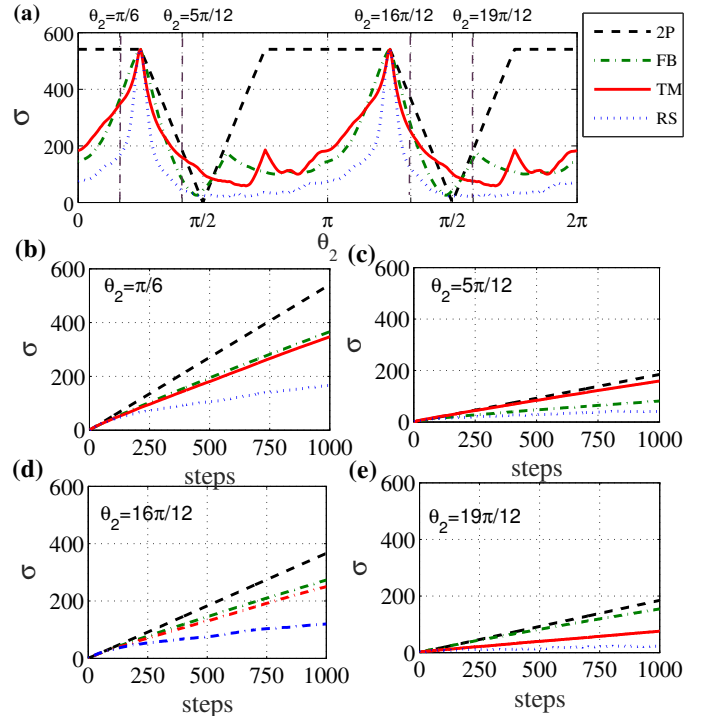


FIG. 14: (Color online). Time dependent coin. (a) Standard deviation at the end of a 1000 step walk as a function of θ_2 with $\theta_1 = \frac{\pi}{4}$. (b)-(e) Standard deviation as a function of time for 1000 steps for different values of θ_2 . The notation used for the sequences are the same as in Fig. 13.

scribes the probability of finding the evolved state within the initial state after some time. Therefore, it is strictly linked to the study of ergodicity and localization of a quantum system and as such has been widely studied in statistical mechanics. On the other hand it is directly related to the Fourier transform of the spectral measure of the evolution operator [44] (and therefore, for an autonomous system, of its infinitesimal generator: the Hamiltonian)

$$|\nu(t)|^2 = \left| \int_{\sigma} d\mu_0(\epsilon) e^{-i\epsilon t} \right|^2, \quad (10)$$

where μ_0 is the measure induced by the initial state $|\psi(0)\rangle$. Therefore its Fourier transform is the measure itself.

A second quantity we will explore is the Cesàro average (time average) of the echo, which is defined as

$$\langle |\nu|^2 \rangle_T = \frac{1}{T} \sum_{t=0}^{T-1} |\nu(t)|^2. \quad (11)$$

A. Position dependent coin operations

In the case of position dependent coin operations the corresponding DTQW is autonomous and therefore its

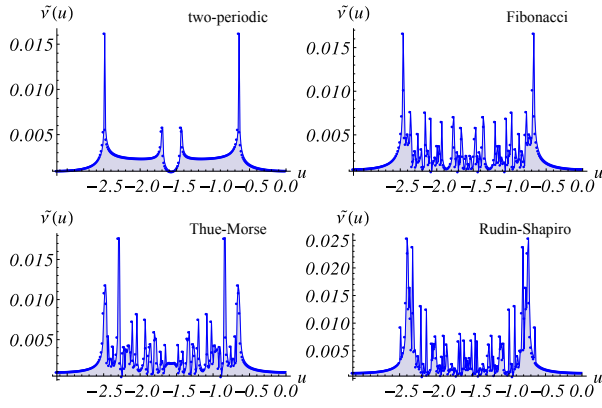


FIG. 15: (Color online). Fourier transform $\tilde{\nu}(u)$ of the survival probability $\nu(t)$ for DTQWs with spatially inhomogeneous coins. The angles chosen are $\theta_1 = \pi/4$ and $\theta_2 = \pi/6$.

asymptotic properties are related to the system's energy spectrum (and to the initial state). We will consider an initial state such that the walker is localized at the centre of the lattice $|x = 0\rangle$ and the coin state is $|\uparrow\rangle$. Since this initial state is localized in real space it is completely delocalized in momentum space and therefore we expect it to have a non-vanishing overlap with nearly all eigenstates of the evolution operator. For the same reason we have chosen an asymmetric coin state. It therefore allows us to explore the full spectrum of the system. Indeed, the peaks in the Fourier transforms $|\tilde{\nu}(u)|$ of the survival amplitude in Fig. 15 closely resemble those of the DOS shown in Fig. 5. This confirms that the chosen initial state is such that each eigenstate is initially occupied to some extent and we can therefore explore the full energy spectrum during the dynamics.

Looking closer at the Fourier transforms shown in Fig. 15 one can note in all of them sharp peaks around $u \approx -2.5$ and $u \approx -0.7$. These peaks are due to the sub-bands generated by the presence of the internal degree of freedom (coin), which can be confirmed by comparing with the corresponding spectra shown in Fig. 4. This is also confirmed by looking at the plot for the two-periodic case where two additional sharp peaks appear at $u \approx -1.7$ and $u \approx -1.4$ which correspond to the further breaking of the corresponding spectrum into new sub-bands due to the modulation of the operators. On the other hand, as expected, the remaining part is continuous and has no sharp peaks.

Looking at $\tilde{\nu}(u)$ for the aperiodic arrangements we can see that, beside the above mentioned sharp peaks corresponding the breaking of the spectrum into two main sub-bands, a series of sharp peaks exist whose positions are aligned with those of the corresponding DOS shown in Fig. 5. The supports of these peaks belongs to the discrete part of the spectrum [44] and we will in the following determine whether they are pure point or singular continuous.

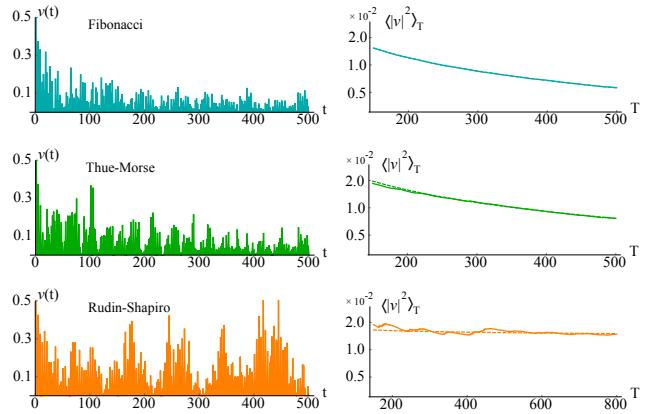


FIG. 16: (Color online). Left: Survival amplitude $\nu(t)$ for different distribution of the coin operators in a DTQWs with spatially aperiodically distributed coin operations. Right: Corresponding Cesàro averages of $|\nu(t)|^2$. The dashed lines are the fit functions.

Given that the survival amplitude in Eq. (10) is the Fourier transform of the measure, one can identify a singular continuous spectrum whenever the conditions (compare with Eq.(2) in Ref. [46] for the averaged correlation function of an observable $f(t)$)

$$\lim_{t \rightarrow \infty} \nu(t) \neq 0 \quad \text{not absolute continuous} \quad (12a)$$

$$\lim_{T \rightarrow \infty} \langle |\nu|^2 \rangle_T = 0 \quad \text{not pure point} \quad (12b)$$

are both satisfied. The first condition ensures the absence of an absolutely continuous part in the spectrum because, according to the RAGE theorem [44], $\lim_{t \rightarrow \infty} \nu(t) = 0$ is a necessary condition for the presence of an absolutely continuous part in the spectrum. The second condition ensures the absence of pure point spectrum due to Wiener's lemma (see lemma 1.1 in [45]). Therefore the simultaneous occurrence of conditions in Eqs. (12a) and (12b) can be interpreted as the spectrum having only singular continuous parts.

On the other hand, the above discussion has shown that in all cases at least four delta-like peaks, corresponding to the splitting of the band into two sub-bands, can be expected and therefore the spectrum has a non-empty discrete component. Bearing this in mind we show in Fig. 16 the asymptotic values of $\nu(t)$ and the corresponding Cesàro averages, $\langle |\nu|^2 \rangle_T$.

It is clear that $\nu(t)$ goes to zero as $t \rightarrow \infty$ only for the two-periodic case. This can be interpreted as the spectrum having an absolutely continuous part (RAGE theorem), which correspond to the continuum inside each of the four sub-bands. In all other cases $\nu(t)$ does not asymptotically vanish and one can therefore expect that the corresponding spectra lack an absolutely continuous part. We notice that among all the Rudin-Shapiro sequence is the one which maintains the highest value at infinite times. The Cesàro averages for all sequences do

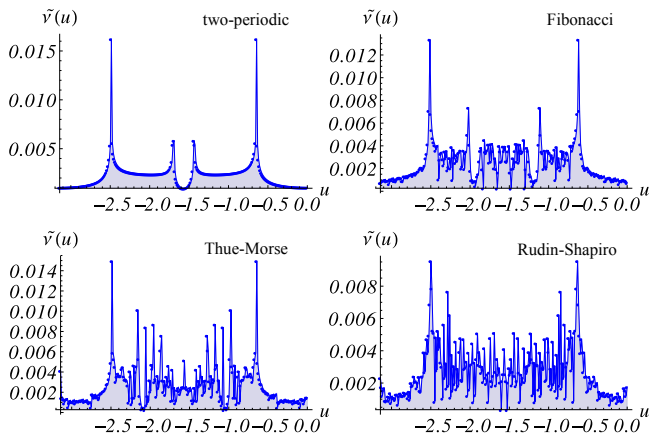


FIG. 17: (Color online). Fourier transform $\tilde{\nu}(u)$ of the survival probability $\nu(t)$ for temporally inhomogeneous DTQWs. The angle chosen are $\theta_1 = \pi/4$ and $\theta_2 = \pi/6$.

not go to zero over the simulated time, which suggests the presence of discrete parts in the spectra and which are due to the splitting into subbands. In order to establish whether or not the Cesàro averages tend to zero at infinity we have fit the data with a power-law function $f(T) = T^\alpha$ with $\alpha < 0$ for the Fibonacci and Thue-Morse cases, whereas for the Rudin-Shapiro we found that the best agreement is with a fitting function of the form $f(T) = e^{\alpha T^\beta}$ with $\alpha < 0$ and $0 < \beta < 1$. Note that, in order to counter the localization effects from the Rudin-Shapiro sequences, we have simulated a larger number of steps to get a better accuracy for the parameters α and β . As it can be seen from the right hand side of Fig. 16 in the Fibonacci and Thue-Morse cases the fit gives a very good agreement and the Cesàro average which decays algebraically to zero. On the other hand for the Rudin-Shapiro case the decay is slower due to localisation effects and in particular we found $\beta = (0.013 \pm 0.001)$. This localisation might be useful for applications such as quantum memories using DTQW [47].

Due to the asymptotic decay of the Cesàro average we can therefore conclude that the spectrum of a DTQW with spatially distributed coin operations has a singular continuous component only (beside the discrete component introduced by the presence of the internal degree of freedom of the coin).

B. Time dependent coin operations

In the case of time dependent coin operations the asymptotic behavior is characterized by the spectrum of the asymptotic evolution operator as discussed in Sec. IV. The Fourier transform of the survival amplitude $\tilde{\nu}(u)$ is shown in Fig. 17 and has a form similar to the spatial case discussed above. However, the peaks in $\tilde{\nu}(u)$ are not similar to the ones in the corresponding DOS of the

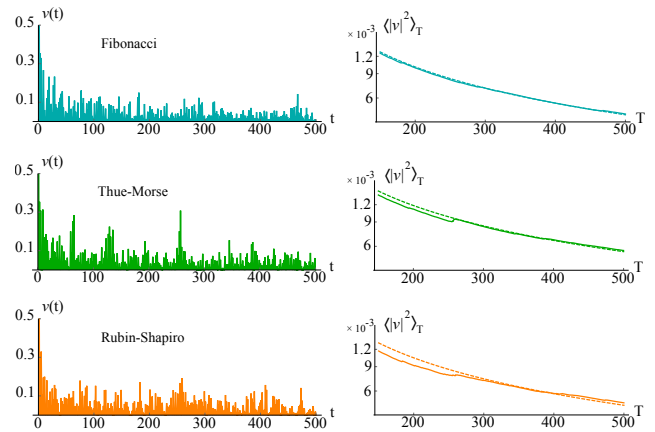


FIG. 18: (Color online). Survival amplitude $\nu(t)$ for different distribution of the coin operators in a DTQWs with spatially aperiodically distributed coin operations. Right: Corresponding Cesàro averages of $|\nu(t)|^2$. The dashed lines are the fit functions.

asymptotic evolution operator, which is shown in Fig. 8. Nevertheless, signatures of the presence of aperiodic order is clearly visible in the sharp spikes and in the self-similar character of $\tilde{\nu}(u)$.

It is therefore interesting to again look at the behavior of the survival amplitude and its Cesàro average. From the left hand side of Fig. 18 we see that the survival amplitude does not go to zero for the large times considered and for all sequences, which allows us to conclude that the corresponding energy spectra do not possess an absolutely continuous part.

Looking at the Cesàro average (right hand side of Fig. 18) we observed that in the temporal case the best fit is a power-law of the form $f(T) = \alpha T^\beta$ for all instances. It is interesting that the Rudin-Shapiro case, which was the slowest to converge to zero for large T in the spatial case, now behaves similarly to the more delocalized walks. Indeed, as it can be observed in Fig. 12, for the case of the temporal Rudin-Shapiro distribution of the coin operations, the wave-packet spreads more than in the case of a spatial Rudin-Shapiro distribution. Therefore, one can conclude that also for temporal distributions the system has a singular continuous spectrum.

VII. CONCLUSIONS

In this work we have presented the study of DTQW with different configuration of aperiodic sequences of position and time dependent coin operations. Analysing the dynamics of the different aperiodic walks by studying the energy spectrum, the standard deviation of the probability distribution, and their asymptotic behavior we have shown that the DTQW using a Fibonacci sequence, which has pure point spectrum, and a Rudin-Shapiro sequence, which has continuous spectrum, are

closer to DTQW with periodic sequence (diffusive spreading) and random sequence (localization), respectively. Quantum walks using Thue-Morse sequences, which have a singular-continuous spectrum, comprise of both, diffusing and localized component in the dynamics. This establishes that quantum walks are an interesting playground to study the interplay between singular continuous spectra and quantum effects and in particular their competition in the transport properties in quantum systems.

VIII. ACKNOWLEDGMENTS

NLG thanks F. Plastina for useful discussions. NLG and LD acknowledge financial support by MIUR through

FIRB Project No. RBFR12NLNA002. NLG acknowledges financial support by the EU Collaborative project QuProCS (Grant Agreement 641277). CMC acknowledge support from DST through Ramanujan Fellowship grant number SB/S2/RJN-192/2014. This work was supported by the Okinawa Institute of Science and Technology Graduate University.

-
- [1] Y. Aharonov, L. Davidovich, and N. Zagury, Quantum random walks, *Phys. Rev. A* **48**, 1687 (1993).
 - [2] E. Farhi and S. Gutmann, Quantum computation and decision trees, *Phys. Rev. A* **58**, 915 (1998).
 - [3] S.E. Venegas-Andraca, Quantum walks: a comprehensive review, *Quantum Information Processing* **11**, 1015 (2012).
 - [4] J. Kempe, Quantum random walks - an introductory overview, *Contemporary Physics* **44**, 307 (2003).
 - [5] A.M. Childs, Universal computation by quantum walk, *Phys. Rev. Lett.* **102**, 180501 (2009).
 - [6] N.B. Lovett, S. Cooper, M. Everitt, M. Trevers, and V. Kendon, Universal quantum computation using the discrete-time quantum walk, *Phys. Rev. A* **81**, 042330 (2010).
 - [7] A. Schreiber, K.N. Cassemiro, V. Potocek, A. Gábris, I. Jex, and Ch. Silberhorn, Decoherence and Disorder in Quantum Walks: From Ballistic Spread to Localization, *Phys. Rev. Lett.* **106**, 180403 (2011).
 - [8] C.M. Chandrashekar, Disordered-quantum-walk-induced localization of a Bose-Einstein condensate, *Phys. Rev. A* **83**, 022320 (2011).
 - [9] T. Kitagawa, M.S. Rudner, E. Berg, and E. Demler, Exploring topological phases with quantum walks, *Phys. Rev. A* **82**, 033429 (2010).
 - [10] D.A. Meyer, From quantum cellular automata to quantum lattice gases, *J. Stat. Phys.* **85**, 551 (1996).
 - [11] G. Di Molfetta, M. Brachet, and F. Debbasch, Quantum walks as massless Dirac fermions in curved space-time, *Phys. Rev. A* **88**, 042301, (2013).
 - [12] C.M. Chandrashekar, Two-component Dirac-like Hamiltonian for generating quantum walk on one-, two- and three-dimensional lattices, *Scientific Reports* **3**, 2829 (2013).
 - [13] G. Di Molfetta, M. Brachet, F. Debbasch, Quantum walks in artificial electric and gravitational fields, *Physica A* **397**, 157 (2014).
 - [14] C.M. Chandrashekar, S. Banerjee and R. Srikanth, Relationship between quantum walks and relativistic quantum mechanics, *Phys. Rev. A* **81**, 062340 (2010).
 - [15] J. Du, H. Li, X. Xu, M. Shi, J. Wu, X. Zhou, and R. Han, Experimental implementation of the quantum random-walk algorithm, *Phys. Rev. A* **67**, 042316 (2003).
 - [16] C.A. Ryan, M. Laforest, J.C. Boileau, and R. Laflamme, Experimental implementation of a discrete-time quantum random walk on an NMR quantum-information processor, *Phys. Rev. A* **72**, 062317 (2005).
 - [17] H. Schmitz, R. Matjeschk, Ch. Schneider, J. Glueckert, M. Enderlein, T. Huber, and T. Schaetz, Quantum Walk of a Trapped Ion in Phase Space, *Phys. Rev. Lett.* **103**, 090504 (2009).
 - [18] F. Zähringer, G. Kirchmair, R. Gerritsma, E. Solano, R. Blatt, and C.F. Roos, Realization of a Quantum Walk with One and Two Trapped Ions. *Phys. Rev. Lett.* **104**, 100503 (2010).
 - [19] M. Karski, L. Förster, J. Choi, A. Steffen, W. Alt, D. Meschede, and A. Widera, Quantum walk in position space with single optically trapped atoms, *Science* **325**, 174 (2009).
 - [20] M. Genske, W. Alt, A. Steffen, A.H. Werner, R.F. Werner, D. Meschede, and A. Alberti, Electric Quantum Walks with Individual Atoms, *Phys. Rev. Lett.* **110**, 190601 (2013).
 - [21] B. Do, M.L. Stohler, S. Balasubramanian, D.S. Elliott, C. Eash, E. Fischbach, M.A. Fischbach, A. Mills, and B. Zwickl, Experimental realization of a quantum quincunx by use of linear optical elements, *Opt. Soc. Amer. B* **22**, 499 (2005).
 - [22] M.A. Broome, A. Fedrizzi, B.P. Lanyon, I. Kassal, A. Aspuru-Guzik, and A.G. White, Discrete Single-Photon Quantum Walks with Tunable Decoherence, *Phys. Rev. Lett.* **104**, 153602 (2010).
 - [23] A. Nayak and A. Vishwanath, Quantum walk on the line, DIMACS Technical Report, 2000-43 (2001).
 - [24] P.W. Anderson, Absence of diffusion in certain random lattices, *Phys. Rev.* **109**, 1492 (1958).
 - [25] C.M. Chandrashekar, Disorder induced localization and enhancement of entanglement in one- and two-dimensional quantum walks, arXiv:1212.5984 (2012).
 - [26] P. Ribeiro, P. Milman, and R. Mosseri, Aperiodic quantum random walks, *Phys. Rev. Lett.* **93**, 190503 (2004).
 - [27] A. Romanelli, The fibonacci quantum walk and its classical trace map, *Physica A* **388**, 3985 (2009).
 - [28] C. Ampadu, Limit theorems for the fibonacci quantum

- walk, arXiv:1108.5198 (2011).
- [29] J.D. Joannopoulos, P.R. Villeneuve and S. Fan, Photonic crystals: putting a new twist on light, *Nature* **386**, 143 (1997).
- [30] Z.V. Vardeny, A. Nahata, and A. Agrawal, Optics of photonic quasicrystals, *Nature Photonics* **7**, 177 (2013).
- [31] D. Shechtman, I. Blech, D. Gratias, and J.W. Cahn, Metallic phase with long-range orientational order and no translational symmetry, *Phys. Rev. Lett.* **53**, 1951 (1984).
- [32] M. Kohmoto, C. Kadanoff, and C. Tang, Localization Problem in One Dimension: Mapping and Escape, *Phys. Rev. Lett.* **50**, 1870 (1983).
- [33] R. Merlin, K. Bajema, R. Clarke, F.Y. Juang, and P.K. Bhattacharya, Quasiperiodic GaAs-AlAs Heterostructures, *Phys. Rev. Lett.* **55**, 1768 (1985).
- [34] R. Riklund, M. Severin, and Y. Liu, The Thue-Morse aperiodic crystal, a link between the Fibonacci quasicrystal and the periodic crystal, *Int. J. Mod. Phys. B* **01**, 121 (1987).
- [35] M.S. Vasconcelos and E.L. Albuquerque, Transmission fingerprints in quasiperiodic dielectric multilayers, *Phys. Rev. B* **59**, 11128 (1999).
- [36] B.L. Burrows and K.W. Sulston, Measurement of disorder in non-periodic sequences, *J. Phys. A: Math. Gen.* **24**, 3979 (1991).
- [37] V. Berthe, Conditional entropy of some automatic sequences, *J. Phys. A: Math. Gen.* **27**, 7993 (1994).
- [38] L.S. Levitov, Localization-Delocalization Transition for One-Dimensional Alloy Potentials, *Europhys. Lett.* **7**, 343 (1988).
- [39] J.M. Luck, Cantor spectra and scaling of gap widths in deterministic aperiodic systems, *Phys. Rev. B* **39**, 5834 (1989).
- [40] A. Suto, Singular continuous spectrum on a cantor set of zero Lebesgue measure for the Fibonacci Hamiltonian, *J. Stat. Phys.* **56**, 525 (1989).
- [41] J.-M. Gambaudo and P. Vignolo, Brillouin zone labelling for quasicrystals, *New J. Phys.* **16**, 043013 (2014).
- [42] N. Lo Gullo, L. Vittadello, M. Bazzan, and L. Dell'Anna, Equivalence classes of Fibonacci lattices and their similarity properties, *Phys. Rev. A* **94**, 023846 (2016).
- [43] C.M. Chandrashekar, R. Srikanth, and R. Laflamme, Optimizing the discrete time quantum walk using a SU(2) coin, *Phys. Rev. A* **77**, 032326 (2008).
- [44] Y. Last, Quantum dynamics and decompositions of singular continuous spectra, *J. Funct. An.* **142**, 406 (1996).
- [45] M. Queffelec, *Substitution Dynamical Systems: Spectral Analysis [Second Edition]*, *Lecture Notes in Mathematics* 1294, Springer-Verlag Berlin Heidelberg (2010).
- [46] A.S. Pikovsky, M.A. Zaks, U. Feudel, and J. Kurths, Singular continuous spectra in dissipative dynamics, *Phys. Rev. B* **52**, 285 (1995).
- [47] C.M. Chandrashekar and Th. Busch, Localized quantum walks as secured quantum memory, *Europhys. Lett.* **110**, 10005 (2015).